

Structure formation dynamics in drawing silica photonic crystal fibres

Wenyu WANG (✉)¹, Ghazal Fallah TAFTI¹, Mingjie DING¹, Yanhua LUO¹, Yuan TIAN¹, Shuai WANG^{1,2}, Tomasz KARPISZ³, John CANNING^{1,4}, Kevin COOK^{1,4}, Gang-Ding PENG (✉)¹

¹ Photonics and Optical Communications, School of Electrical Engineering and Telecommunications, University of New South Wales (UNSW) Sydney, 2052, Australia

² Henan Key Laboratory of Laser and Opto-Electric Information Technology, School of Information Engineering, Zhengzhou University, Zhengzhou 450052, China

³ Warsaw University of Technology, 00-665, Warsaw, Poland

⁴ Interdisciplinary Photonics Laboratories (iPL), School of Electrical and Data Engineering, University of Technology Sydney, and School of Chemistry, The University of Sydney, NSW 2007 & 2006, Australia

© Higher Education Press and Springer-Verlag GmbH Germany, part of Springer Nature 2018

Abstract The special features of photonic crystal fibres (PCFs) are achieved by their air hole structures. PCF structure is determined and formed by its origin preform design and drawing process. Therefore, structure formation dynamics in drawing PCF is important for the fabrication of PCF achieving desirable structure and thus the intended feature. This paper will investigate structure formation dynamics of PCF drawing in relation to key parameters and conditions, such as hole dimension, temperature, pressure, etc.

Keywords photonic crystal fibre (PCF), structure formation, hole dimension, hole position, hole shift

1 Introduction

Photonic crystal fibres (PCFs) have attracted lots of interest as they could provide special features that conventional fibres cannot achieve [1], such as near-endlessly single mode [2], strong optical nonlinear effects [3] and high-birefringence [4]. Therefore, they are widely used in (but not limited to) fibre lasers [5–7], fibre sensors [8,9], and nonlinear devices [3,10].

PCF features are mainly determined by the geometry structure of the air holes such as hole dimension, hole shape and hole position [2]. However, hole deformation may happen in the drawing process due to the viscosity and surface tension of the material. Therefore, it is essential to

understand the structure formation dynamics in drawing PCF to achieve the original hole structure in the preform by accurate controlling drawing conditions like furnace temperature T_d , drawing pressure P_d , feeding rate V_f , and drawing rate V_d .

To understand the structure formation in drawing process, much theoretical analysis work has been done. The drawing process modeling of PCF [11,12] related to hole collapse was setup in Ref. [13]. Fitt et al. [14,15] carried out the single capillary drawing approach under isothermal condition, and the stability of drawing capillaries has been reported in Refs. [16,17]. The control of hole expansion was theoretically studied [18] and the method of predicting hole dimension disregarding viscosity was provided [19]. Furthermore, in the drawing process, the transverse radiative heat transfer inside the silica preform was numerically analyzed [12,20,21]. In addition to these theoretical studies, several experiments were carried out to explore proper PCF drawing parameters. For example, the relationships of the hole dimension and the spacing pitch between pressure [22], temperature, feeding rate, feeding time, and capillary wall thickness were reported [23–26]. However, directly taking advantage of these results is not practical due to the structural and design differences in drawing facilities. Thus, in order to customize the PCF drawing in our own draw tower, the relationship between the structure formation dynamics and pressure P_d at different T_d was primarily studied for the normal PCF and the high-birefringence PCF [27,28]. Following the previous work, this paper will provide a further analysis of the structure formation dynamics including hole position and hole centre shift in the drawing process.

2 PCF structure and structure parameters

2.1 Basic structure parameters

The cross section images of the PCF and its preform are shown in Figs. 1(a) and 1(c) and the structural parameters of the PCF and its preform are described in Figs. 1(b) and 1(d). The hole diameters of fibre and preform are defined as $2r_{h,f}$ and $2r_{h,p}$. The radii of fibre and preform are denoted as $r_{o,f}$ and $r_{o,p}$. r_f is the distance between the centre of the fibre and that of the hole, and r_p is the distance between the centre of the preform and that of the hole. The hexagonal rings from inner to outer are named as Ring 1, Ring 2, Ring 3, and Ring 4, respectively. Since some holes in Ring 4 are fully collapsed, only the holes in Ring 1, 2 and 3 will be considered and described in this work. Three red circled holes marked as H_1 , H_2 and H_3 at Ring 1, 2 and 3 in Figs. 1(b) and 1(d) are typically selected to represent the structure formation of the holes in each ring.

2.2 Scale factor of hole-outer diameter ratio of fibre to preform R

For describing the collapse degree of the air hole, a scale

factor R is defined as

$$R = \frac{2r_{h,f}/(2r_{o,f})}{2r_{h,p}/(2r_{o,p})} = \frac{r_{h,f}/r_{o,f}}{r_{h,p}/(2r_{o,p})}, \quad (1)$$

where numerator term represents the hole-outer diameter ratio of fibre, and denominator term is the hole-outer diameter ratio of preform. According to the definition in Eq. (1), the change of air holes in PCF has the following four cases:

when $R = 0$, holes are fully collapsed and $r_{h,f} = 0$;

when $R < 1$, holes are partially collapsed;

when $R > 1$, holes are expanded;

when $R = 1$, holes keep the same ratio as those in the preform without any collapse or expansion (internal air pressure is balanced with the surface tension and drawing shear force). Here, P_d is defined as the optimal pressure, P_o .

2.3 Relative position of the hole in fibre R_f

To study the relationship between the structure formation and hole position, the relative position of the hole in fibre R_f is defined in Eq. (2):

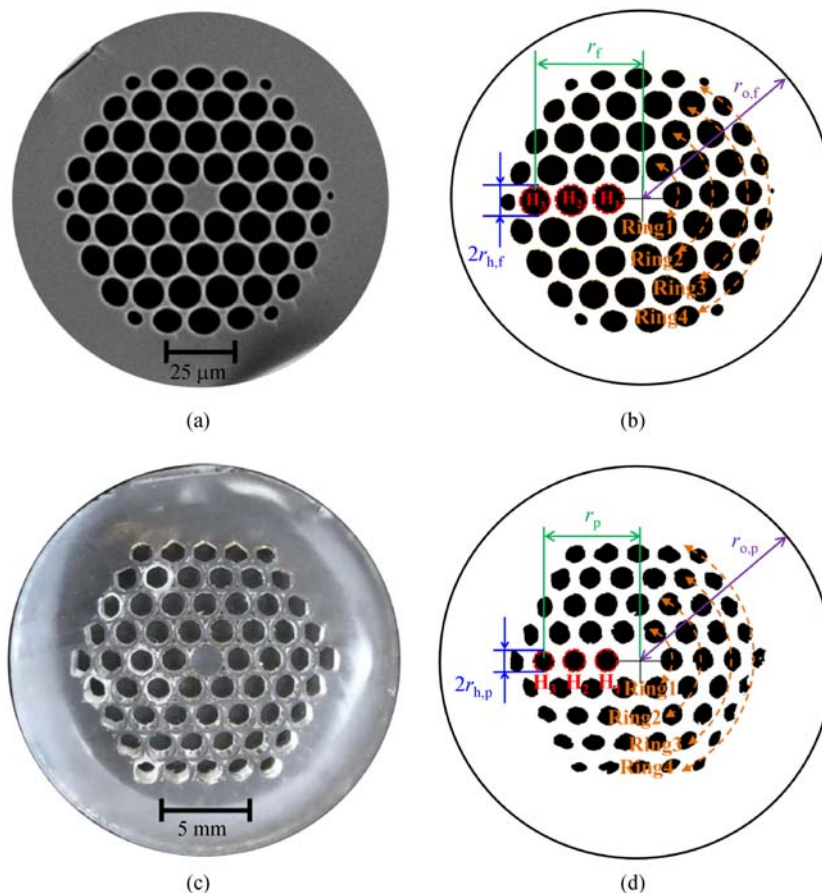


Fig. 1 Cross section images of a fabricated PCF (a) and its preform (c). The basic structural parameters are labeled in (b) for the PCF and (d) for the preform. The colors of (b) and (d) are calibrated for clearer views

$$R_f = \frac{r_f}{r_{o,f}} \quad (2)$$

2.4 Relative position of the hole in preform R_p

Similarly, the relative position of the hole in preform (R_p) is defined in Eq. (3):

$$R_p = \frac{r_p}{r_{o,p}} \quad (3)$$

3 PCF fabrication results and discussion

The PCF preform used was assembled by stacking a series of capillaries forming the hexagon shape with four rings and jacketing these capillaries with a silica tube. The inner diameter D_{inner} and outer diameter D_{tube} of the jacket tube are 18.93 and 24.97 mm, and the ratio of outer to inner diameter of the capillary is 1.32. The space between the capillaries and jacket tube was filled with solid rods for two reasons: 1) stabilizing the stacked hexagon PCF structure; 2) avoiding an excessive collapse of the holes at Ring 4 caused by high temperature at outer layer in the drawing process [1]. Then the stacked preform was fused on a lathe to relax the tolerance in drawing process by removing the interstitial area so that only lattice structure was concerned. The outer diameter of the fused preform D_{preform} is 21.5 mm which means 25.8% of preform was collapsed (the area of cross section). Finally, the fused preform was drawn into fibres with furnace temperature $T_d = 1860^\circ\text{C}$ and $T_d = 1870^\circ\text{C}$, drawing pressure $P_d = 2.8\text{--}18.5\text{ mbar}^1$,

feeding rate $V_f = 0.5\text{ mm/min}$, and drawing rate $V_d = 15\text{ m/min}$.

3.1 Scale factor R vs. drawing pressure P_d at different furnace temperature T_d

In our previous work [27], the relationship between drawing pressure P_d and scale factor R was discussed according to the cross section image scanned by the electron microscope shown in Figs. 2(a) and 2(b). Seen from Fig. 2(a), when $P_d = 2.8\text{ mbar}$, the R of H_1 , H_2 and H_3 are measured to be 0.43, 0.36 and 0.29 at $T_d = 1860^\circ\text{C}$. These less than one R values indicate the collapse of the holes. With the rise of P_d to 9 mbar, the R of each hole grows close to 1, which means a balanced pressure is nearly provided at the boundary between the air hole and the glass. Finally, when P_d is changed up to 12 mbar, the R of each hole surpasses 1. In this case, the holes are supposed to be expanded according to the definition of R . Therefore, the rule of R vs. P_d can be concluded as: 1) when P_d is set in a low region, the scale factor R moves towards zero due to insufficient drawing pressure to resist the collapse tension; 2) when increasing the P_d , the high drawing pressure will overcome the collapse tension and blow up the hole, resulting in the increase of R .

In addition, it has been found that the optimal pressure P_o increases with the radial distance from the centre, which is H_1 (8.5 mbar) $<$ H_2 (9.1 mbar) $<$ H_3 (10.2 mbar). Normally lower viscosity under higher T_d leads to more collapse. As a result of a thermal gradient, a hole in the outer ring has a significantly higher temperature environment and a lower viscosity than the one in the inner ring. So that, as the experimental results show, a hole in the outer

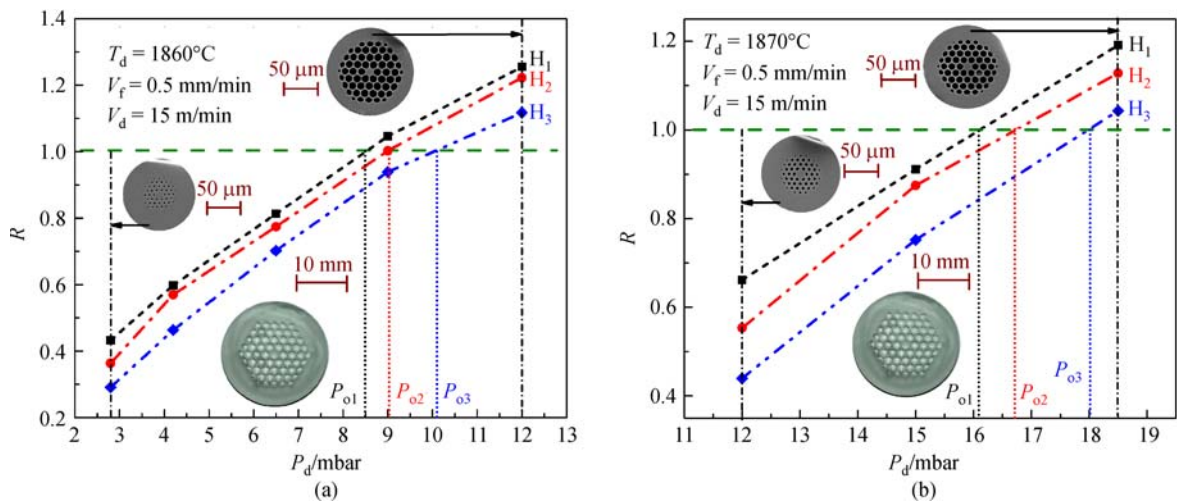


Fig. 2 Dependences of the scale factor R on the drawing pressure P_d for holes H_1 , H_2 and H_3 . The results are shown for two furnace temperatures: (a) 1860°C and (b) 1870°C . Cross-section images of the preform and four PCFs with different drawing conditions are illustrated. The green dash lines represent $R = 1$. The optimal pressures of holes H_1 , H_2 and H_3 are marked as P_{o1} , P_{o2} , P_{o3}

1) 1 mbar = 100 Pa

ring requires considerably increased P_d to maintain the structure. Besides, a strong temperature dependence of P_o is confirmed by comparing the optimal pressure P_o in Figs. 2(a) and 2(b): when the furnace temperature T_d increased by 10°C , the P_o of each hole increases by the ratio of 1.77–1.89 [27].

3.2 Relative position of hole in fibre R_f vs. drawing pressure P_d at different furnace temperature T_d

The optimum PCF drawing is to achieve the targeted structure directly scaled down from its preform. However, the material migration always exists in PCF drawing due to the un-balance between the drawing pressure and the collapse tension. It will not only change the hole dimension, but also the position of hole in PCF regarding with that in the preform. The variation of the position of hole in PCF regarding with that in preform means that the movement of a hole in PCF is not in the proposition to the position of the hole in preform. In order to have a better control of the position of the holes in the PCF drawing process, the relative position of hole in fibre (R_f) is introduced as Eq. (2) and its dependences on the drawing pressure and furnace temperature is further studied.

In Fig. 3, the R_f of three tracked holes as a function of the drawing pressure P_d of 2.8–18.5 mbar at different furnace temperature T_d are plotted. The R_f of all three holes is almost increased (i.e., moving away from the center) with the increase of P_d . The H_3 hole has the most significant movement with the P_d because it has the largest slope m of R_f to P_d . Compared with the relative position of hole in preform R_p (indicated as orange dash lines), the movement of the hole in the inner layer is less. Such phenomena might

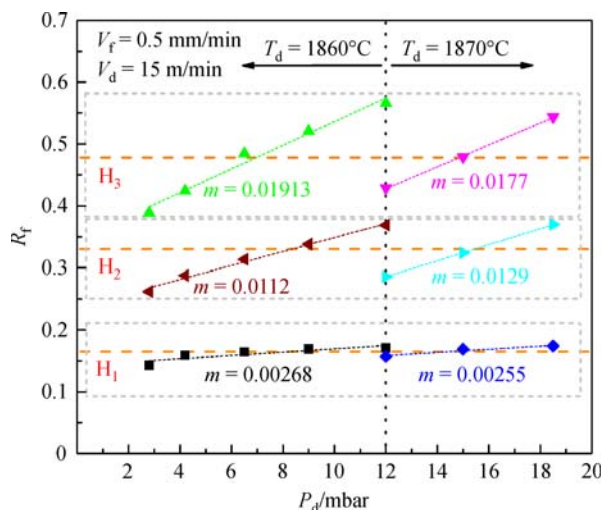


Fig. 3 Dependences of relative position of the hole in PCF (R_f) upon the drawing pressure P_d for holes H_1 , H_2 and H_3 at different temperature: 1860°C (left part to the dotted line) and 1870°C (right part to the dotted line). The orange dash lines represent the relative position of holes in the preform (R_p). m is the slope of R_f to P_d

be attributed to two reasons: 1) the effect of hole H_3 located in the outer ring includes the additive effect from the inner rings; 2) the holes in the outer ring have less restraint than those in the inner rings. For the latter reason, the hole H_1 needs to push hole H_2 and H_3 if it tends to move outward, meanwhile, it is restricted by the high material viscosity in the centre of the PCF when it is going to move towards the centre of the fibre.

When the P_d is increased to 9 mbar at $T_d = 1860^\circ\text{C}$, an optimal condition is obtained for the hole H_2 , because the R_f of hole H_2 is 0.338, which is only 0.005 larger than the relative position in preform R_p . In the meantime, the difference between the R_f (0.169) and the R_p (0.167) of H_1 is very small at this drawing condition as well. When the temperature is increased by 10°C , the R_f is found to be lower than that at 1860°C with the same $P_d = 12$ mbar. Considering that the optical property in PCF is largely decided by the inner layers [29], the optimal drawing condition at 1870°C is suggested to be 15 mbar according to the R_f of H_1 and H_2 . Hence, drawing conditions of 9 mbar at 1860°C and 15 mbar at 1870°C are favorable settings for maintaining the hole positions in preform after PCF drawing.

3.3 Scale factor R vs. relative position of hole in fibre R_f

As discussed above, both of the scale factor R and relative position of hole in fibre R_f can be significantly affected by the drawing pressure and furnace temperature. Thereby, it is meaningful to investigate how these two parameters react to the drawing condition correspondingly and search for a drawing condition to optimize R and R_f simultaneously. In Fig. 4, the relationship of R and R_f calculated for H_1 , H_2 and H_3 are plotted with different drawing conditions.

Under the same drawing pressure P_d and furnace temperature T_d , the R drops with increasing R_f , which means the hole at inner layer has less collapse ($0 < R < 1$) or more expansion ($R > 1$) than that at outer layer. Such correlation between the R and R_f holds for any investigated drawing condition shown in Figs. 4(a) and 4(b). Knowing that the optimal R is 1 and the optimal R_f equals to the relative position of hole in the preform R_p , the optimal R and R_f are plotted by dash lines accordingly. Thus, it is easy to understand that three intersections are the optimal points for three holes in Figs. 4(a) and 4(b). Therefore, an optimal drawing condition is $P_d = 9$ mbar and $T_d = 1860^\circ\text{C}$, where all R values of three holes have the smallest difference with each other, and the R_f of H_1 and H_2 locate close to their best position.

In an ideal situation, the R and R_f should fulfill all optimal conditions. However, the scale factor R has more or less dependence on the R_f , indicating that it is difficult to make all of the R in each ring equal to one at the same time. Hence, one strategy to solve this problem is to reduce the dependence of R on R_f . In Fig. 5, the slope s of the R to the

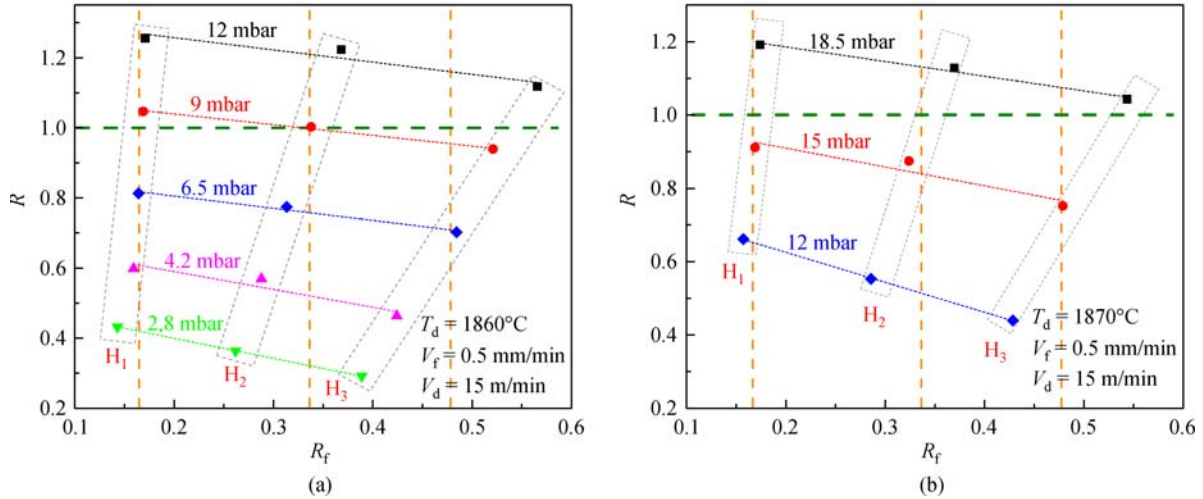


Fig. 4 Dependence of scale factor R on the relative position of hole in the fibre R_f for holes H_1 , H_2 and H_3 at (a) $T_d = 1860^\circ\text{C}$ and (b) $T_d = 1870^\circ\text{C}$. The orange dash lines represent the relative position of hole in the preform R_p . The green dash lines represent $R = 1$

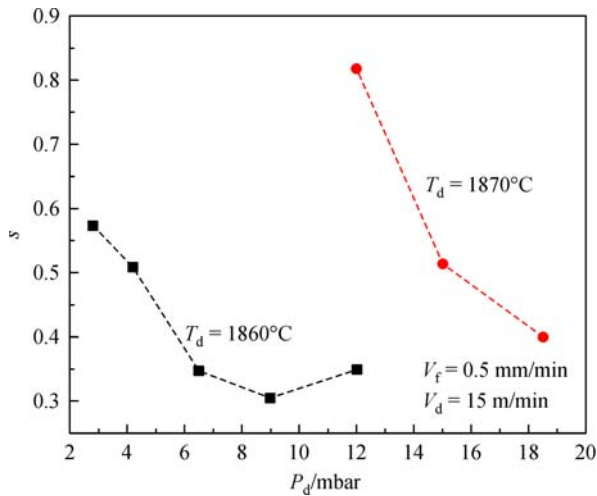


Fig. 5 Dependence of the slope s of the scale factor R to the relative position of hole in the fibre R_f upon the drawing pressure P_d for holes H_1 , H_2 and H_3 at different furnace temperatures

R_f with same drawing condition is calculated to represent the degree of the dependence of the R on the R_f . At both T_d , slope s tends to decrease with increasing P_d and is likely to converge to some range (0.3–0.35 at 1860°C). This result implies that the strength of the dependence of R on R_f can be reduced by increasing the P_d . In other words, the holes at each ring will have a similar deformation behavior under high drawing pressure. Moreover, by decreasing the temperature from 1870°C to 1860°C , the s drops significantly from 0.82 to 0.35 with drawing pressure of 12 mbar showing a great dependence of s on the furnace temperature. Based on these analyses, one can have a low R dependence on R_f by carefully lowering the furnace temperature and obtain an optimal R by adjusting the P_d

afterward. However, attention on the corresponding variation of R_f on the P_d needs to be paid as well.

4 Conclusion

Optical features of PCFs are determined by the air hole structure, formed by its preform design and the following control of the conditions in PCF drawing process. Two new structure parameters—scale factor R and relative position of hole in fibre R_f have been introduced to assess the structure formation compared with its preform. The relationships between scale factor R , relative position of hole in fibre R_f and drawing conditions, including drawing pressure P_d and furnace temperature T_d , have further been investigated by a series of PCFs drawn under different drawing conditions. To maintain the PCF structure, the optimal pressure is required, which shows a strong temperature dependence, while to maintain the hole position of PCF as the preform, two sets of the drawing conditions are favorable. This investigation predicts that there exists an optimal condition to achieve perfect PCF structure without hole collapse/expansion as well as hole shift as the design.

Acknowledgements We thank AFRL, HEL-JTO and AFOSR/AOARD for providing the funding for this work under grant number FA2386-16-1-4031. T. K. thanks the support of the European Community project—PANTHER (Pacific Atlantic Network for Technical Higher Education and Research).

References

1. Buczynski R. Photonic crystal fibers. Acta Physica Polonica A, 2004, 106(2): 141–167

2. Birks T A, Knight J C, Russell P S J. Endlessly single-mode photonic crystal fiber. *Optics Letters*, 1997, 22(13): 961–963
3. Stone J M. Photonic crystal fibres and their applications in the nonlinear regime. Dissertation for the Doctoral Degree. Bath: University of Bath, 2009
4. Michie A, Canning J, Lyytikäinen K, Aslund M, Digweed J. Temperature independent highly birefringent photonic crystal fibre. *Optics Express*, 2004, 12(21): 5160–5165
5. Wadsworth W, Percival R, Bouwmans G, Knight J, Russell P. High power air-clad photonic crystal fibre laser. *Optics Express*, 2003, 11(1): 48–53
6. Cook K, Canning J, Holdsworth J, Dewhurst C. Stable CW single-mode photonic crystal fiber DFB ring laser. *Journal of Electronic Science and Technology of China*, 2008, 6(4): 442–444
7. Groothoff N, Canning J, Ryan T, Lyytikäinen K, Inglis H. Distributed feedback photonic crystal fibre (DFB-PCF) laser. *Optics Express*, 2005, 13(8): 2924–2930
8. Chen T, Chen R, Jewart C, Zhang B, Cook K, Canning J, Chen K P. Regenerated gratings in air-hole microstructured fibers for high-temperature pressure sensing. *Optics Letters*, 2011, 36(18): 3542–3544
9. Michie A, Canning J, Bassett I, Haywood J, Digweed K, Ashton B, Stevenson M, Digweed J, Lau A, Scandurra D. Spun elliptically birefringent photonic crystal fibre for current sensing. *Measurement Science & Technology*, 2007, 18(10): 3070–3074
10. Cook K, Canning J, Holdsworth J. Birefringent Bragg gratings in highly-nonlinear photonic crystal fiber. *Journal of Electronic Science and Technology of China*, 2008, 6(4): 426–428
11. Lyytikäinen K. Numerical simulation of a specialty optical fibre drawing process. In: *Proceedings of 27th Australian Conference on Optical Fibre Technology*. Australia: Sydney, 2002, 134–136
12. Lyytikäinen K, Råback P, Ruokolainen J. Numerical simulation of a specialty optical fibre drawing process. In: *Proceedings of 4th International ASME/JSME/KSME Symp. Computational Technologies for Fluid/Thermal/Chemical/Stress System with Industrial Applications*. Canada: Vancouver, BC, 2002, 267–275
13. Wynne R M. A Fabrication process for microstructured optical fibers. *Journal of Lightwave Technology*, 2006, 24(11): 4304–4313
14. Fitt A D, Furusawa K, Monro T M, Please C P, Richardson D J. The mathematical modelling of capillary drawing for holey fibre manufacture. *Journal of Engineering Mathematics*, 2002, 43(2-4): 201–227
15. Fitt A D, Furusawa K, Monro T M, Please C P. Modeling the fabrication of hollow fibers: capillary drawing. *Journal of Lightwave Technology*, 2001, 19(12): 1924–1931
16. Yarin A L, Gospodinov P, Roussinov V I. Stability loss and sensitivity in hollow fiber drawing. *Physics of Fluids*, 1994, 6(4): 1454–1463
17. Gospodinov P, Yarin A L. Draw resonance of optical micro-capillaries in non-isothermal drawing. *International Journal of Multiphase Flow*, 1997, 23(5): 967–976
18. Wadsworth W, Witkowska A, Leon-Saval S, Birks T. Hole inflation and tapering of stock photonic crystal fibres. *Optics Express*, 2005, 13(17): 6541–6549
19. Chen Y, Birks T A. Predicting hole sizes after fibre drawing without knowing the viscosity. *Optical Materials Express*, 2013, 3(3): 346–356
20. Lyytikäinen K, Zagari J, Barton G, Canning J. Heat transfer in a microstructured optical fibre preform. In: *Proceedings of 11th International Plastic Optical Fibers Conference*. Japan: Tokyo, 2002, 53–56
21. Lyytikäinen K, Zagari J, Barton G, Canning J. Heat transfer within a microstructured polymer optical fibre preform. *Modelling and Simulation in Materials Science and Engineering*, 2004, 12(3): S255
22. Lyytikäinen K, Canning J, Digweed J, Zagari J. Geometry control of air-silica structured optical fibres using pressurisation. In: *Proceedings of Microwave and Optoelectronics Conference*. Brazil: Parana, 2003, 1001–1005
23. Lyytikäinen K J. Control of complex structural geometry in optical fibre drawing. Dissertation for the Doctoral Degree. Sydney: University of Sydney, 2004, 157–176
24. Chen Y. Hole control in photonic crystal fibres. Dissertation for the Doctoral Degree. Bath: University of Bath, 2013, 52–61
25. Guo T Y, Luo S Q, Li H L, Jian S L. Control of the fabrication parameters during the fabrication of photonic crystal fibers. *Acta Physica Sinica*, 2009, 58(9): 6308–6315
26. Lyytikäinen K, Canning J, Digweed J, Zagari J. Geometry control of air-silica structured optical fibres. In: *Proceedings of Optical Internet & Australian Conference on Optical Fibre Technology*. Australia: Melbourne, 2003, 137–140
27. Wang W, Karpisz T, Tafti G, Canning J, Cook K, Luo Y, Peng G. Optimal pressure for tuning the lattice structure of photonic crystal fibre. In: *Proceedings of 3rd Australian and New Zealand Conference on Optics and Photonics*. New Zealand: Queenstown, 2017, Paper 141
28. Tafti G, Wang W, Karpisz T, Canning J, Cook K, Luo Y, Wang S, Peng G. Fabrication and structure of H-Bi micro-structured optical fibres. In: *Proceedings of 3rd Australian and New Zealand Conference on Optics and Photonics*. New Zealand: Queenstown, 2017, Paper 142
29. Hoo Y L, Jin W, Shi C, Ho H L, Wang D N, Ruan S C. Design and modeling of a photonic crystal fiber gas sensor. *Applied Optics*, 2003, 42(18): 3509–3515



Ms. **Wenyu Wang** received her B.E. degree in measuring and control technology and instrumentation from Changchun University of Technology, Changchun, China, in 2011 and M.E. degree in telecommunication from University of Malaya, Kuala Lumpur, Malaysia, in 2015. She is currently a M.E. student in the Photonics and Optical Communication

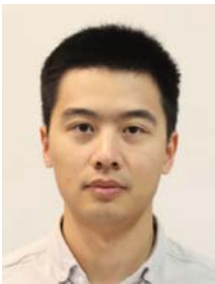
Group in the School of Electrical Engineering and Telecommunications at the University of New South Wales, Sydney, Australia. Her research mainly focuses on the fabrication of hi-birefringence spun photonic crystal fibres, drawing conditions control on the structure formation of photonic crystal fibres, and optical properties of bismuth-erbium co-doped fibres.

Email: wenyu.wang@student.unsw.edu.au



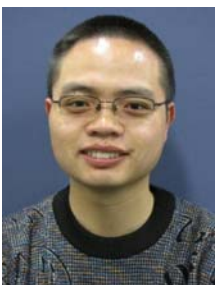
Ms. **Ghazal Fallah Tafti** received her B.Sc. degree in electrical engineering from Isfahan University of Applied Sciences and Technology, Iran, in 2008 and worked as an Aircraft Engineer in Iran-Airline for four years. During her B.Sc. study, she conducted a research on the phone towers and antennas and their environmental impacts. She is currently a M.Sc. student in the School of Electrical Engineering and Telecommunications at the University of New South Wales, Australia. Her research mainly focuses on the fabrication of high-birefringence micro-structured fibres (Hi-Bi MSF) and the effects of drawing parameters on the structure of the micro-structured fibres.

Email: g.fallahtafti@student.unsw.edu.au



Mr. **Mingjie Ding** received his B.E. degree in mechanical engineering from the Shanghai University, Shanghai, China in 2007 and M.E. degree in information processing from the Tokyo Institute of Technology, Tokyo, Japan in 2013. He joined in the Photonics and Optical Communication Group in the School of Electrical Engineering and Telecommunications at the University of New South Wales, Sydney, Australia as a doctoral candidate in 2014. His research interests include functional optical fibre communication, nonlinear optics sensing, application of ultrasonic levitation and deep learning. So far he has published over 6 refereed journal papers and 7 international conference papers as first author. He received an award from Naito foundation for dispatch of young researchers abroad in 2012. He won the best student paper award in the 21st International Congress on Acoustics in 2013. He is a student member of OSA.

Email: m.ding@student.unsw.edu.au



Dr. **Yanhua Luo** received his B.E and Ph. D. degrees from University of Science and Technology of China (UTSC) in 2004 and 2009, respectively. During his Ph.D. study, he had spent one and a half years in School of Electrical Engineering and Telecommunications at University of New South Wales (UNSW) as a practicum student. His research interest is functional photonics materials, fibres and devices, including rare earth based photonic materials, photo-responsive photonic materials, POF and silica fiber-design, fabrication & applications, etc. He has made many contributions to photonics materials and devices. So far he has held 2 China patents and co-authored 88 refereed journal papers, 70 conference papers and 3 book chapters on these subjects. Dr. Luo started working as a postdoctoral researcher in USTC in 2009 and then in UNSW in 2010. Currently, he works as a lab manager of

Photonics and Optical Communication Laboratory at University of New South Wales assisting Prof. Gang-Ding Peng to maintain the National Joint Fibre Facility at UNSW and develop the next generation functional specialty optical fibers and their devices.

Email: yanhua.luo1@unsw.edu.au



Mr. **Yuan Tian** received his B.Sc. degree in optical information science and technology from the School of Physics, Qingdao University, Qingdao, China, in 2016. He is currently pursuing the M.E. degree in the telecommunication engineering in School of Electrical Engineering and telecommunications, University of New South Wales, Sydney, Australia. His research is focused on the design and fabrication of the photonic crystal fibres and their applications, fundamental study of high-birefringence, and fabrication of micro-structured fibres.

Email: yuan.tian1@student.unsw.edu.au



Mr. **Shuai Wang** received his M.E. degree in control engineering from the School of Control Engineering, Huazhong University of Science and Technology, Wuhan, China, in 2011. He is currently pursuing the Ph.D. degree in the information and communication engineering in School of Information Engineering, Zhengzhou University, Zhengzhou, China. Now he is in the joint training in the Photonics and Optical Communication Group in School of Electrical Engineering and Telecommunications, University of New South Wales, Sydney, Australia. His research is focused on the design and fabrication of the photonic crystal fibres and their applications, fundamental study of refractive index sensors, and fabrication of micro-structured fibres.

Email: shuai.wang5@student.unsw.edu.au



Mr. **Tomasz Karpisz** received his B.Sc. degree in electronics, telecommunication and computer engineering in 2013, and M. Sc. in electronics in 2015 from Warsaw University of Technology. Both degrees concerned simulation of linear and non-linear photonic crystal fibres properties. During his B.Sc. and M.Sc. studies, he worked for three years as a technologist in Institute of Electronic Materials Technology, Warsaw, Poland till 2015. He was responsible for design, numerical simulation and properties evaluation as well as production process of photonic crystal fibre made in institute. During his M.Sc. studies, he worked for three years as an engineer in QWED, Warsaw, Poland till 2016. During this period, he was responsible for development of methods

for characterization of bituminous materials using resonant techniques as well as designing and construction of power supply system and control unit for microwave applicator for heating bituminous surface. He was working as an intern in Boulder Environmental Sciences and Technology in 2015 being responsible for designing microwave components. During his PhD study, he had spent half a year in School of Electrical Engineering and Telecommunications at University of New South Wales as a practicum student. So far he is co-author of 6 refereed journal papers and 8 conference papers. Currently, he works on PhD diploma at field of electronics designing high quality resonators for evaluation of electromagnetic properties of low loss samples and liquids.

Email: tkarpisz@ire.pw.edu.pl



Prof. **John Canning** is with the School of Electrical and Data Engineering at the University of Technology Sydney (UTS), and runs the interdisciplinary Photonics Laboratories (*iPL*). He is a Conjoint professor at the School of Electrical Engineering and Telecommunications, University of New South Wales. He has cofounded several companies as well as helped to develop the technology of several others. He is a Fellow of SPIE and the Optical Society of America and received the 2012 OSA's Outstanding Reviewer Award and the 2017 OSA David Richardson Medal. His students have won best paper awards and other prizes, including in 2007 the IEEE Photonics Society for top global students (Cicero Martelli) and a Hitachi Innovation Prize for Agriculture in 2016. He has co-founded and supported several start-ups most recently Australian Sensing and Identification (AusSI) Systems. He has been consultant for a number of companies and individuals over the years in technology, commercialisation and intellectual property generation as well as mentoring. He has been an Otto Monsted Professor at the Danish Technical University, Denmark 2004, and a Villum Kann Rasmussen Professor at iNANO, Aarhus University, Denmark 2007, Science Without Borders Professor at UTFPR, Brazil 2014 – 2017, is part of a Program 111 at UESTC, Chengdu, China since 2014 and has been a Guest Professor at the Laser Institute Shandong Academy of Sciences, China. He has been an Expert Member of the University of Sydney's Latin Regional Advisory Committee and an Advisor to the China and India activities of the University. He has over 700 peer reviewed journal and conference papers and has lodged more than 35 patents and has been a plenary, keynote and invited speaker at more than 30 events and is on the International Steering Committee for OFS, the world's largest optical fibre sensing conference and APOS, the largest Asia Pacific optical sensing conference. He has also been chair and TPC committee member on a range of conferences in photonics including BGPP in Sydney in 2016.

His interests include research student mentoring, science,

photonics, photonic sensing, photonic devices and the photonic IoT, materials, surface plasmons, smart materials, smart sensing, smart device instrumentation, lasers, optical fibres and waveguides, organic photonics, new technologies and applications of technology.

Email: John.Canning@uts.edu.au



Dr. **Kevin Cook** received his Ph.D. degree in physics from Heriot-Watt University, Edinburgh, United Kingdom, in 2005. Currently, he is a research fellow in the School of Electrical and Data Engineering (SEDE). Alongside Prof. John Canning and team, he forms part of the interdisciplinary Photonics Laboratories (*iPL*). Kevin's research interests span many areas of engineering and science with a particular focus on photonics, optical communications, optical sensing, Bragg gratings, nanotechnology and 3D printing. Some of his major achievements include demonstrating the world's first optical fibre fabricated from a 3D printed preform, pioneering work that has spurred other 3D-printing firsts such as fabrication of rib optical waveguides and structured optical fibres that guide in visible and near infrared. Kevin also holds strong research interest in optical fibre smart sensing networks that can be deployed for the monitoring of mines, railways, bridges, buildings and other civil infrastructure. Kevin has also worked extensively on the development of smartphone-based sensing instruments such as spectrometers, laser profilers and fluorimeters, all of which feed directly into the so-called "internet of things" (IoT).

Email: Kevin.Cook@uts.edu.au



Prof. **Gang-Ding Peng** received his B.Sc. degree in physics from Fudan University, Shanghai, China, in 1982, and M.Sc. degree in applied physics and Ph.D. degree in electronic engineering from Shanghai Jiao Tong University, Shanghai, China, in 1984 and 1987, respectively. From 1987 through 1988, he was a lecturer of Shanghai Jiao Tong University. He was a postdoctoral research fellow in the Optical Sciences Centre of the Australian National University, Canberra, from 1988 to 1991. He has been working with UNSW since 1991, was a Queen Elizabeth II Fellow from 1992 to 1996 and is currently a Professor in the same university. He is a fellow and life member of both OSA and SPIE. His research interests include specialty silica and polymer optical fibres, optical fibre and waveguide devices, optical fibre sensors and nonlinear optics. So far, he has published more than 200 refereed journal papers and more than 200 conference papers, and co-authored more than 10 book chapters on these subjects.

Email: g.peng@unsw.edu.au